

Performance study of Na₃PO₄-expanded graphite composites for low-temperature thermochemical heat storage[#]

Junfeng Zhou^{2,3}, Shusen Lin^{2,3}, Lisheng Deng^{1,2}, Jun Li^{2,3}, Tao Zeng², Zhen Huang^{2,3}, Hongyu Huang^{2,3*}

1 Tianjin Key Laboratory of Integrated Design and On-line Monitoring for Light Industry & Food Machinery and Equipment, Tianjin, 300222, China

2 Guangzhou Institute of Energy Conversion, Chinese Academy of Sciences, Guangzhou 510640, China

3 School of Energy Science and Engineering, University of Science and Technology of China, Hefei, 230026, China
(Corresponding Author: huanghy@ms.giec.ac.cn)

ABSTRACT

Salt hydrate-based thermochemical heat storage is a crucial technology for long-term heat storage. Sodium phosphate stands out due to its high energy storage density, lower dehydration temperature, and low cost. However, its practical application is limited by issues such as deliquescence and agglomeration. In this study, expanded graphite, known for its high thermal conductivity and rich microstructure, was used as the primary matrix. Composites with mass contents of 80%, 60%, and 40% were prepared using the impregnation method. Hydration tests were conducted at 30°C and RH 80% to examine the microstructure, thermal storage properties, and cycling stability of the pure salt and the composites. The results demonstrated that the incorporation of expanded graphite improved the adsorption kinetics of the composites and thermal conductivity mitigated the deliquescent agglomeration of pure salt, and reduced the dehydration temperature. EG80 has a maximum water absorption of 1.24 g/g, an energy storage density of 1081.8 kJ/kg and a thermal conductivity of 2.98 W/(m-K). After 10 storage discharge cycles, the thermal storage density remained above 1000 kJ/kg, indicating good stability.

Keywords: thermochemical energy storage, Na₃PO₄·12H₂O, energy storage density, cycle stability

NONMENCLATURE

Abbreviations

TCES	Thermochemical Energy Storage
ESD	Energy Storage Density
EG	Expanded Graphite

Symbols

m	Mass
---	------

1. INTRODUCTION

In the context of global energy shortages and environmental degradation, the adoption of renewable energy sources is imperative for sustainable development. Despite the projection by the International Energy Agency (IEA) indicated that renewable energy is poised to represent 80 percent of new capacity by 2030[1], the inherent intermittency of sources like solar and wind energy creates a mismatch between supply and demand, posing challenges for their large-scale application [2,3]. Thermochemical Energy Storage (TCES) has become a crucial technology in fields such as renewable energy integration and industrial waste heat recovery. Among the various thermochemical systems, the hydrated salt system has garnered substantial attention due to its low cost, high safety, and lower dehydration temperature [4,5].

Due to the huge heat demand for domestic heating and hot water supply, the integration of high efficiency TCES technologies with building energy efficiency is still to be technically and commercially developed [6]. Low dehydration temperatures are effective in improving solar energy conversion efficiency. Donkers et al. [7] conducted an analysis of thermodynamic data for numerous hydrated salts to assess their suitability for seasonal heat storage in constructed environments. Through screening, they identified 25 salt hydrates that met three specific criteria: an energy storage density exceeding 1.3 GJ/m³, a hydration temperature above 50°C, and a dehydration temperature below 120°C. Among them, SrBr₂·6H₂O and LiOH·H₂O can meet the demand of heating and hot water supply with their high thermal storage density, but their cost issues further limit their applications.

[#] This is a paper for the 16th International Conference on Applied Energy (ICAE2024), Sep. 1-5, 2024, Niigata, Japan.

Recently, Kubota et al. [8] analyzed and evaluated 32 kinds of salts for low-temperature heat storage. They found that $\text{LiOH}\cdot\text{H}_2\text{O}$, $\text{Na}_3\text{PO}_4\cdot 12\text{H}_2\text{O}$ and $\text{Ba}(\text{OH})_2\cdot 8\text{H}_2\text{O}$ exhibited promising potential for TCES, with ESD exceeding 1000 kJ/kg. Clark et al. [9] found that Na_3PO_4 has high ESD under a range of dehydration and hydration conditions. Specifically, volumetric energy density of 296 and 315 kWh/m^3 were observed at dehydration temperatures of 70 and 100 $^\circ\text{C}$, respectively. These findings suggest that Na_3PO_4 is a promising salt under the given conditions. Although the aforementioned hydrated salts demonstrate considerable potential in TCES, they are still subject to limitations, including deliquescence, agglomeration, and poor thermal conductivity.

Relevant studies have demonstrated that the addition of porous media can effectively improve the heat and mass transfer of TCMs. In our work, expanded graphite (EG) was chosen as the porous carrier to enhance the material's thermal conductivity while providing a rich void network to accommodate the salt. Composites with varying loadings (EG80, EG60, and EG40) were prepared by combining $\text{Na}_3\text{PO}_4\cdot 12\text{H}_2\text{O}$ and EG using the melt impregnation method. The thermal storage properties and cycling stability of these composites were subsequently investigated.

2. EXPERIMENTAL

2.1 Synthesis of Na_3PO_4 -EG composite materials

To prevent the hydrolysis of sodium phosphate, melt impregnation was employed to synthesize the composites [10]. **Fig. 1** illustrates a typical synthesis

bottomed flask containing anhydrous ethanol and the temperature is rapidly raised to 80 $^\circ\text{C}$. The purpose of this procedure is to ensure that the $\text{Na}_3\text{PO}_4\cdot 12\text{H}_2\text{O}$ becomes fully molten. This stage is crucial for facilitating the subsequent integration of the EG. Prior to this, the EG is dried overnight in a 200 $^\circ\text{C}$ oven to ensure that any residual moisture is eliminated. The EG was then precisely weighed and added to the molten $\text{Na}_3\text{PO}_4\cdot 12\text{H}_2\text{O}$ mixture in accurate proportions. The composite blend underwent an intensive stirring regimen for 6 hours to encourage comprehensive blending and even distribution of the EG particles within the matrix. Following the conclusion of the blending process, the mixture was allowed to cool to ambient temperature and then filtered to acquire the EG- $\text{Na}_3\text{PO}_4\cdot 12\text{H}_2\text{O}$ composite material. The resultant composites, dependent on the integrated sodium phosphate content, were denoted as EG40, EG60 and EG80, indicating the percentage by weight of the sodium phosphate in the composite.

2.2 Structural and property characterization

The microscopic morphology of TCMs was characterized by field emission scanning electron microscopy (FESEM, S-4800, Hitachi, Japan) with an accelerating voltage of 7kV. X-ray diffractometer (XRD, D8-advance, Bruker, Germany) was used to analyze the phase compositions of EG, composites with different contents and to detect the successful preparation of TCMs. Mercury Indicated Porosimetry (MIP, Autopore V9600, Micrometrics Instrument Corp.) was used to determine the macropores properties of the materials in

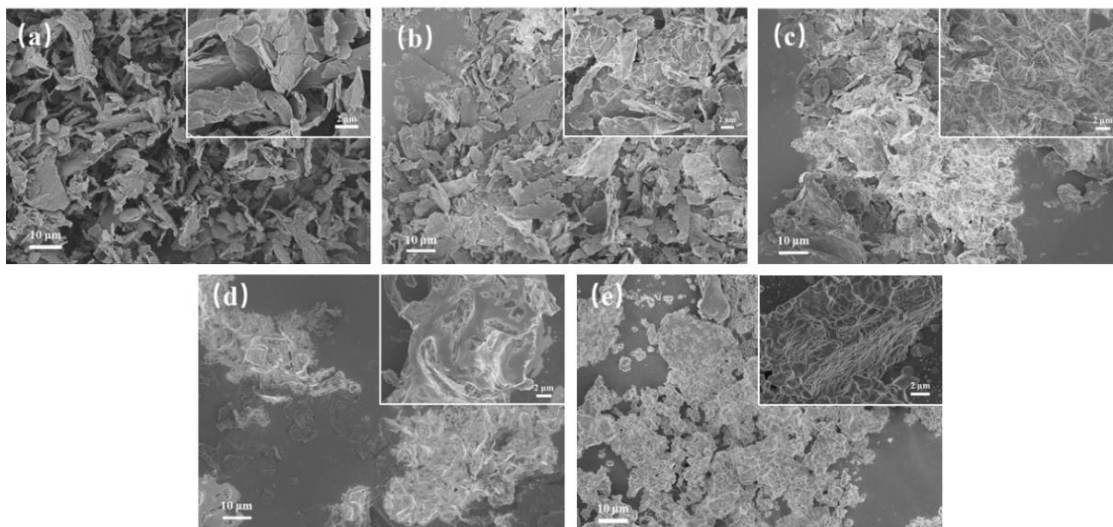


Fig. 1 SEM images of (a) EG; (b) EG 20; (c) EG 40; (d) EG60; (e) $\text{Na}_3\text{PO}_4\cdot 12\text{H}_2\text{O}$

process of Na_3PO_4 -EG composites. Initially, an accurately weighed amount of $\text{Na}_3\text{PO}_4\cdot 12\text{H}_2\text{O}$ is added to a round-

the measurement range of 5-5000 nm. A simultaneous thermal analyzer (TGA/DSC+, METTLER TOLEDO,

Switzerland) was used to measure changes in weight and heat flow during desorption (dehydration) and adsorption (hydration). 5-10 mg of composite TCM was placed in an alumina crucible and heated from 25 °C to 150 °C at a heating rate of 5 °C /min. A hot plate thermal constant analyzer (TPS-2200, Hot Disk Inc., Sweden) was used to determine the thermophysical properties of TCMs.

2.3 Adsorption kinetics performance

A constant temperature and humidity chamber (Labonce-60CH, Labonce Thermostatic Technology Co., Ltd., China) was used to characterize the dynamic adsorption process and the equilibrium adsorption amount of the adsorbent under specified temperature and humidity conditions. A precision electronic balance (AX224ZH, OHAUS, Changzhou, China) with an accuracy of 0.0001 g (range 220 g) was used for static weighing. The temperature was set at 30°C and the RH was 80%.

During the test, about 0.1 g of the sample was taken and placed on a Petri dish ($\varphi 6$) to lay flat for the hydration experiments, and the time step for the balance data acquisition was 10 s. The formula for calculating the equilibrium adsorption per unit adsorption was shown in the following equation:

$$m_{ads} = \frac{m - m_0}{m_0}$$

Where m_{ads} is the unit equilibrium adsorption capacity, g/g; m is the total mass of the adsorbent after water absorption, g; and m_0 is the total mass of the dry composite, g. Provide sufficient detail to allow the work to be reproduced. Methods already published should be indicated by a reference: only relevant modifications should be described.

3. RESULTS AND DISCUSSION

SEM images of EG and Na₃PO₄-EG composites with different contents are shown in **Fig. 1**. As can be seen in (a), EG has a clear lamellar structure that stacks on top of each other to form voids that can accommodate salt. (b)-(d) show the distribution of sodium phosphate in the EG voids of the composites with different contents. It can be seen that Na₃PO₄ in the molten state covers the EG layer, and the EG stacked voids gradually decrease with the increase of Na₃PO₄ content, indicating that more Na₃PO₄ is captured by the pores of EG. In the case of EG80, for example, the molten slurry of sodium phosphate fills in the voids of EG, and the characteristic of EG flakes becomes less obvious. Na₃PO₄ encapsulated in the EG flake increases the contact area with water vapor, which will facilitate the mass and heat transfer of the

composite, which will be discussed in detail later in the article.

Fig. 2 illustrates the XRD patterns of EG, Na₃PO₄, and their composites with varying salt contents. The

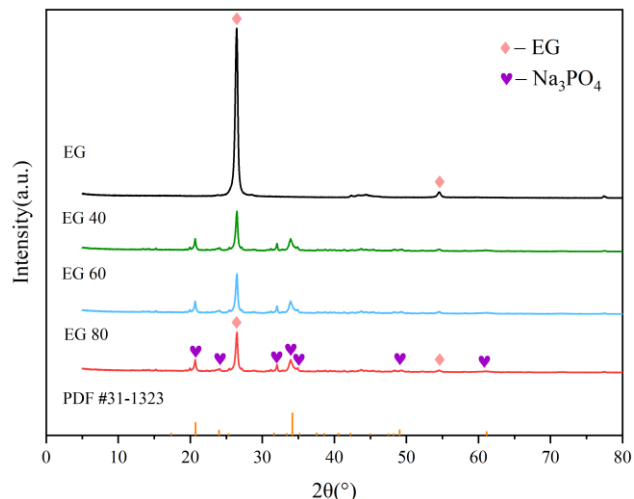


Fig. 2 XRD patterns of samples.

prominent, sharp peak at approximately 26° is indicative of the (002) crystal plane of graphite, a characteristic of EG due to its highly ordered structure. Another diffraction peak located at 54° was revealed which was demonstrated a dominant feature in the XRD patterns of pure EG samples [11]. The peaks of Na₃PO₄ are primarily located at ~20.7°, 23.9°, 31.6°, 34.1°, 35.1°, 49.0°, and 61.1°, which is consistent with the standard card PDF#00-031-1323 in the ICDD crystal database. For the Na₃PO₄-EG composites, their XRD patterns are only related to the crystal structures of Na₃PO₄ and EG. However, the intensity of all peaks in the mixtures decreased compared to the pure components. The absence of new characteristic peaks after mixing of EG and Na₃PO₄ suggests that the composites are formed only by physical bonding without the creation of new substances and have a good chemical compatibility.

The **Table 1** presents a summary of the pore structure parameters of EG and composites. In particular, pure EG exhibits the largest pore volume and average pore diameter of 4.0052 mL/g and 1038.51 nm, respectively. With the increase in salt content, the average pore diameter and pore volume of the composites decreased to varying degrees. For instance, the pore volume of EG80 decreased to 2.3257 mL/g, while the average pore diameter decreased to 527.04 nm in comparison to EG, which exhibited a 42% and 49% reduction, respectively. In general, the specific surface area decreased with the increase in salt content.

Table 1 Microstructure properties of samples.

Samples	Average pore size (nm)	Pore volume (cm ³ /g)	Surface area (m ² /g)
EG80	527.04	2.3257	17.651
EG60	663.18	2.7623	16.661
EG40	888.18	3.1324	14.107
EG	1038.51	4.0052	15.427

In practical TCES systems, the thermal storage performance is largely influenced by the adsorption kinetics and capacity of the material. Since EG cannot adsorb water vapor [12], the water absorbed by the material can be attributed to the hydration of Na₃PO₄. The Fig. 3 depicts the hydration curves for various loadings at 30 °C under RH80%. It is obvious that the equilibrium water absorption of the material increases with the increase of salt loading. The unit equilibrium adsorption amounts of EG80, EG60 and EG40 are 1.24 g/g, 0.72 g/g and 0.46 g/g, and the hydration equilibrium is reached around 240 min, compared with that of the pure salt, which still has not reached equilibrium at 600 min. At this point, the salt hydration went through two stages, the first stage, sodium phosphate and water vapor hydration reaction to form a saturated crystalline

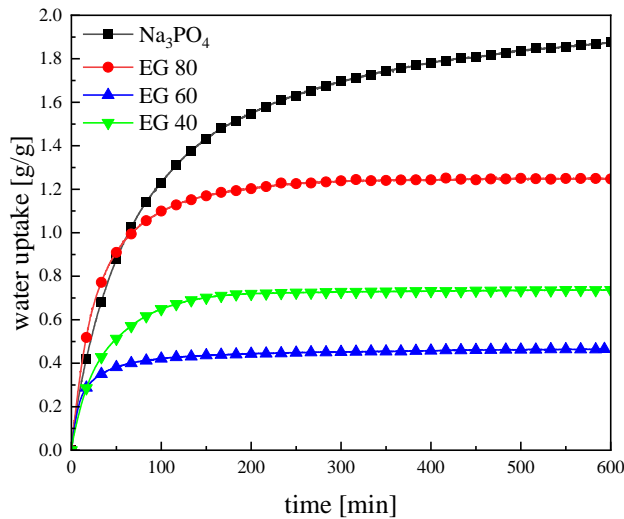


Fig. 3 Water adsorption kinetics of pure salt and composites at 30°C and RH80%

hydrate; the second stage, under high humidity, the salt on the surface absorbs water to form a liquid film continues to absorb water to form a solution until equilibrium. The addition of EG solves the problem of pure salt deliquescence and further improves the hydration kinetics.

TG was used to analyze the dehydration behavior of pure salt and composites, as shown in Fig. 4(a), the composites reached the dehydration equilibrium faster

than the pure salt under the same temperature rise condition, and the fastest rate was observed for EG40, which was attributed to the lowest salt content and less relative equilibrium water absorption. At the same time, the dehydration temperatures of the composites are also

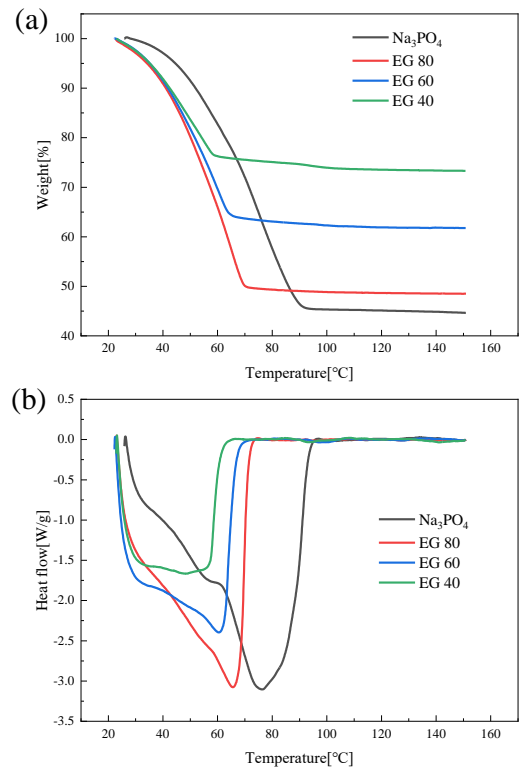


Fig. 4 TG and DSC curves of pure salt and composites at 30°C and RH80%

decreasing, and the temperatures at which the pure salt and the composites EG80, EG60, and EG40 reach the dehydration equilibrium are 92 °C, 70 °C, 65 °C, and 60 °C, respectively. This is 19%, 29% and 34% lower compared to pure salt. This indicates that the composites only require lower temperatures to complete the desorption, which is due to the enhanced thermal conductivity of the material due to the addition of expanded graphite [13].

The DSC results are depicted in Fig. 4(b). The highest heat absorption peak of the composites shifted significantly to the left, indicating that the addition of EG accelerated the dehydration process and lowered the dehydration temperature, consistent with TG analysis results. As the salt content increased, the heat absorption peaks became progressively narrower. The ESD of the pure salt and composite materials was calculated by integrating the peak area, as shown in Table 2. The ESD increased with higher salt content, with the pure salt reaching 1261.4 kJ/kg. The ESD for EG80, EG60, and EG40 were 1081.8 kJ/kg, 797.6 kJ/kg, and 542.9 kJ/kg, respectively, corresponding to 86%, 63%,

and 43% of the pure salt. The thermal conductivity of pure salt and composite materials was measured using a thermal constant analyzer. The lowest thermal conductivity was found in pure salt at 0.52 W/(m·K). With the addition of EG, the thermal conductivities of the composites EG80, EG60, and EG40 were 2.98 W/(m·K), 4.12 W/(m·K), and 5.11 W/(m·K), respectively, representing increases of 5.7, 7.8, and 9.8 times compared to pure salt.

Table 2 Energy storage density and thermal conductivity of pure salt, EG and composites with different loadings

	Na ₃ PO ₄	EG80	EG60	EG40	EG
ESD (kJ/kg)	1261.4	1081.8	797.6	542.9	-
Thermal conductivity [W/(m·K)]	0.52	2.98	4.12	5.11	6.78

Cyclic stability is also a crucial criterion for evaluating TCMs. The best sample, EG80, was hydrated in a chamber at 30°C and 80% RH, and dried at 60°C in a vacuum drying oven before testing. The ESD of the samples was assessed by TG-DSC after hydration experiments. **Fig. 5** illustrates the changes in ESD and equilibrium water absorption over 10 cycles. Generally, the thermal storage properties of the material decrease with an increasing number of cycles. The thermal storage performance of EG80 still maintains a ESD of 1000 kJ/kg after 20 cycles, indicating that EG80 retains stable performance throughout the cycling process.

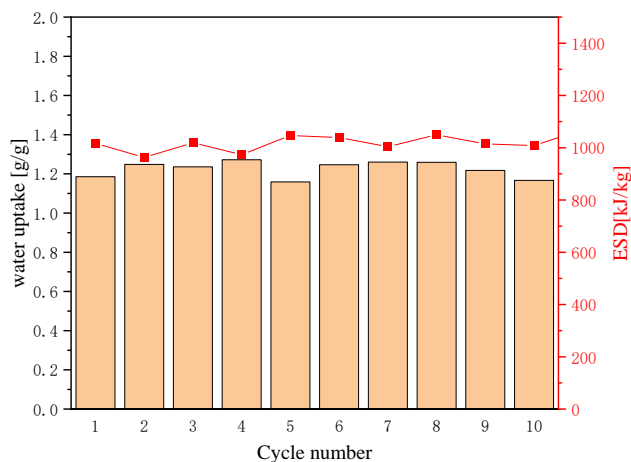


Fig. 5 Stability of the cycle water uptake and ESD of EG80 composite

4. CONCLUSIONS

In this study, a novel composite material for low-temperature thermochemical heat storage was successfully developed using the melt impregnation method. Sodium phosphate hydrated salt served as the

heat storage material, while EG functioned as the primary matrix. The structure and properties of the resulting composite were thoroughly investigated, leading to the following specific conclusions:

1) The incorporation of EG effectively enhanced the mass and heat transfer properties of the material. The macroporous structure of EG accommodated a greater amount of salt, allowing for uniform distribution within the interlayer through purely physical interactions. The composite, EG80, exhibited a thermal conductivity of 2.977 W/(m·K), which is 5.7 times higher than that of the pure material.

2) At 30°C and RH 80%, EG80 achieved the highest ESD of 1081.8 kJ/kg. Even at low humidity (50% RH), EG80 maintained a high ESD of 935.9 kJ/kg, which is 86.5% of its value at 80% RH.

3) After 20 consecutive storage-exothermic cycles, the equilibrium water uptake of EG80 generally showed a decreasing trend. However, the ESD remained above 1000 kJ/kg, demonstrating the material's stability over repeated cycles.

In conclusion, this research successfully developed a new thermochemical material based on sodium phosphate for low-temperature thermochemical storage. The composite material prepared via melt impregnation demonstrated stable properties and promising application potential. Future studies will focus on evaluating the performance of this composite material at the reactor level to provide technical support for practical implementations.

ACKNOWLEDGEMENT

This work is supported by the National Natural Science Foundation of China Grants Program (No. 52176091) and Open Fund of Tianjin Key Laboratory of Integrated Design and On-line Monitoring for Light Industry & Food Machinery and Equipment (2022LIMFE01).

REFERENCE

- [1] IEA (2024), CO₂ Emissions in 2023, IEA, Paris <https://www.iea.org/reports/co2-emissions-in-2023>
- [2] Rahman, M. M., Oni, A. O., Gemechu, E., & Kumar, A. (2020). Assessment of energy storage technologies: A review. *Energy Conversion and Management*, 223, 113295.
- [3] Liu, J., Hu, C., Kimber, A., & Wang, Z. (2020). Uses, cost-benefit analysis, and markets of energy storage systems for electric grid applications. *Journal of Energy Storage*, 32, 101731.

- [4] Yan, T. S., Li, T. X., Xu, J. X., & Chao, J. W. (2020). Understanding the transition process of phase change and dehydration reaction of salt hydrate for thermal energy storage. *Applied Thermal Engineering*, 166, 114655.
- [5] Gordeeva, L. G., & Aristov, Y. I. (2019). Adsorptive heat storage and amplification: New cycles and adsorbents. *Energy*, 167, 440-453.
- [6] Li, W., Klemeš, J. J., Wang, Q., & Zeng, M. (2020). Development and characteristics analysis of salt-hydrate based composite sorbent for low-grade thermochemical energy storage. *Renewable Energy*, 157, 920-940.
- [7] Donkers, P. A. J., Sögütoglu, L. C., Huinink, H. P., Fischer, H. R., & Adan, O. C. G. (2017). A review of salt hydrates for seasonal heat storage in domestic applications. *Applied energy*, 199, 45-68.
- [8] Kubota, M., Matsumoto, S., Matsuda, H., Huang, H. Y., He, Z. H., & Yang, X. X. (2014). Chemical heat storage with LiOH/LiOH-H₂O reaction for low-temperature heat below 373 K. *Advanced Materials Research*, 953, 757-760.
- [9] Clark, R. J., Gholamibozanjani, G., Woods, J., Kaur, S., Odukomaiya, A., Al-Hallaj, S., & Farid, M. (2022). Experimental screening of salt hydrates for thermochemical energy storage for building heating application. *Journal of Energy Storage*, 51, 104415.
- [10] Lin, S., Deng, L., Li, J., Kubota, M., Kobayashi, N., & Huang, H. (2024). Preparation and properties of activated carbon-based Na₃PO₄ composites for low-temperature thermochemical heat storage. *Energy*, 301, 131592.
- [11] Fu, W., Zou, T., Liang, X., Wang, S., Gao, X., Zhang, Z., & Fang, Y. (2018). Thermal properties and thermal conductivity enhancement of composite phase change material using sodium acetate trihydrate-urea/expanded graphite for radiant floor heating system. *Applied Thermal Engineering*, 138, 618-626.
- [12] Tao, Z., Wang, H., Li, X., Liu, Z., & Guo, Q. (2017). Expanded graphite/polydimethylsiloxane composites with high thermal conductivity. *Journal of Applied Polymer Science*, 134(21).
- [13] Groen, J. C., Peffer, L. A., & Pérez-Ramírez, J. (2003). Pore size determination in modified micro-and mesoporous materials. Pitfalls and limitations in gas adsorption data analysis. *Microporous and mesoporous materials*, 60(1-3), 1-17.